INSTITUTE OF PHYSICS PUBLISHING JOURNAL OF PHYSICS: CONDENSED MATTER

J. Phys.: Condens. Matter **13** (2001) 6195–6202 PII: S0953-8984(01)21276-4

The Jahn–Teller effect and electron–phonon interaction in $La_{0.25}Ca_{0.75}Mn_{1-x}Cr_xO_3$

H-D Zhou, G Li, H Chen, R-K Zheng, X-J Fan and X-G Li

Structure Research Laboratory, Department of Materials Science and Engineering, University of Science and Technology of China, Hefei 230026, People's Republic of China

E-mail: lixg@ustc.edu.cn (X-G Li)

Received 23 January 2001, in final form 29 May 2001
Published 29 June 2001
Online at stacks.iop.org/JPhysCM/13/6195

Abstract

The ultrasonic (longitudinal and transverse) velocities and the transport and magnetic properties of polycrystalline $La_{0.25}Ca_{0.75}Mn_{1-x}Cr_xO_3$ ($x = 0$, 0.03, 0.05, and 0.07) have been studied systematically. It was found that with increasing Cr content, the resistivity increases, the charge-ordering transition temperature T_{CO} shifts to low temperature, and the magnetic moment of the system is strengthened. From the temperature dependence of the ultrasonic velocities, one can establish that the Jahn–Teller energy and phonon exchange constant decrease with increasing Cr content.

1. Introduction

Colossal magnetoresistance (CMR) in the manganese oxides $Ln_{1-x}A_xMnO_3$ with mixed Mn^{3+}/Mn^{4+} valence has become a focus of recent studies in view of their special electronic and magnetic properties as well as the potential applications. The double-exchange theory of Zener [1] has been used to explain the coexistence of ferromagnetism and metallicity of the samples near $x \sim 0.3$. However, it was found that the double-exchange interaction alone cannot explain the colossal magnetoresistance, and some other mechanisms were proposed such as that of the polaron theory [2] which can be used to explain the intriguing charge-ordering (CO) phenomena observed in richly hole-doped CMR materials. The CO behaviour has manifestations in many experimental measurements, including a sharp increase of dc resistivity [3], an inflection of the specific heat and thermal conductivity [4, 5], structural changes [6], a strong magnetic field dependence of the oxygen isotope [7], and phase separation [8, 9]. In previous work [3, 6, 10], the ultrasonic technique has proven to be a particularly successful means of studying CO behaviour, as a sensitive probe. It has been found that around the charge-ordering transition temperature T_{CO} the abnormal changes of velocities and attenuations are closely related to the strong electron–phonon coupling in the charge-ordered system [6]. Despite all these previous studies, how the change of the Mn^{3+}/Mn^{4+} ratio and the ferromagnetism of the charge-ordered

 © 2001 IOP Publishing Ltd Printed in the UK

system influence the Jahn–Teller (J–T) effect and electron–phonon interaction remains unclear. In this work, we studied the effect of Cr substitution for Mn on the ultrasonic, transport, and magnetic properties of the $La_{0.25}Ca_{0.75}Mn_{1-x}Cr_xO_3$ ($x = 0$, 0.03, 0.05, and 0.07) charge-ordered system, and found that Cr doping changes the J–T effect and the electron–phonon coupling.

2. Experimental procedure

Polycrystalline samples of $La_{0.25}Ca_{0.75}Mn_{1-x}Cr_xO_3$ ($x = 0$, 0.03, 0.05, and 0.07) were prepared by a standard solid-state reaction method. A stoichiometric mixture of high-purity La_2O_3 (baked above 800 °C for 2 h), $CaCO_3$, MnO_2, and Cr_2O_3 was ground and calcined at 1200 °C for 24 h. The reactant underwent intermediate regrinding and was pressed into pellets for sintering at 1300 °C for 24 h. The fabricated samples are of high compaction; the density is about 4.63 g cm^{-3}, near to the theoretical density 4.99 g cm^{-3}, and the pore occupancy ratio is only 7.2%. These pellets were then polished to maintain a thickness of 4 mm and the alignment of the top and bottom planes was about 5×10^{-5} rad. Powder x-ray diffraction patterns were recorded by a MacScience MAXP18AHF diffractometer using Cu Kα radiation. The XRD patterns show that all samples are of single cubic phase. The resistivity was measured by a standard four-probe technique. The zero-field-cooled (ZFC) and field-cooled (FC) magnetizations were measured in an external magnetic field of 50 G using a commercial superconducting quantum interference device magnetometer. The ultrasonic velocity and attenuation measurements were performed on the Matec-7700 series by means of a conventional pulsed-echo technique. Longitudinal and transverse wave pulses were generated by 10 MHz X-cut and Y-cut quartz transducers. Noneg Stock oil was used to couple the transducer and samples.

3. Results and discussion

Figure 1(a) shows the temperature dependencies of the resistivities of polycrystalline samples of $La_{0.25}Ca_{0.75}Mn_{1-x}Cr_xO_3$ ($x = 0$, 0.03, 0.05, and 0.07). One can see that the resistivity shows a semiconductor-like transport behaviour without a semiconductor-to-metal transition, and increases slightly with Cr doping. As shown in figure 1(b), the resistivity, plotted as $d(\ln \rho)/d(T^{-1})$, has an abnormal peak, which corresponds to the charge-ordering transition of the system according to Ramirez *et al* [3]. The charge-ordering transition temperature T_{CO} moves to low temperatures as the Cr content increases; see the inset of figure 1(b). Around T_{CO} the ordering of localized polarons originating from the J–T effect cause a sharp increase of the resistivity.

The variations of the magnetizations with temperature of the system are shown in figure 2. Both the zero-field-cooled (ZFC) and field-cooled (FC) magnetizations in an external magnetic field of 50 G are depicted. For $x = 0$, the ZFC magnetization (M_{ZFC}) first increases as temperature decreases, then arrives at a maximum value around $T_{CO} \sim 205$ K, below which M_{ZFC} decreases as temperature further decreases. Other samples show similar magnetic behaviours. It can be seen from the ZFC and FC curves that in the low-temperature range the increases of the magnetizations with increasing Cr concentration indicate that the ferromagnetism of the system is strengthened, which is similar to the case for the $Pr_{0.5}Ca_{0.5}Mn_{1-x}Cr_xO_3$ system reported on by Raveau *et al* [11, 12]. Figure 3 shows the Cr content dependence of the maximum ZFC magnetization values ($M_{ZFC\,max}$) derived from the ZFC magnetization curves in figure 2. Since Cr^{3+} is isoelectronic with Mn^{4+}, the ferromagnetic

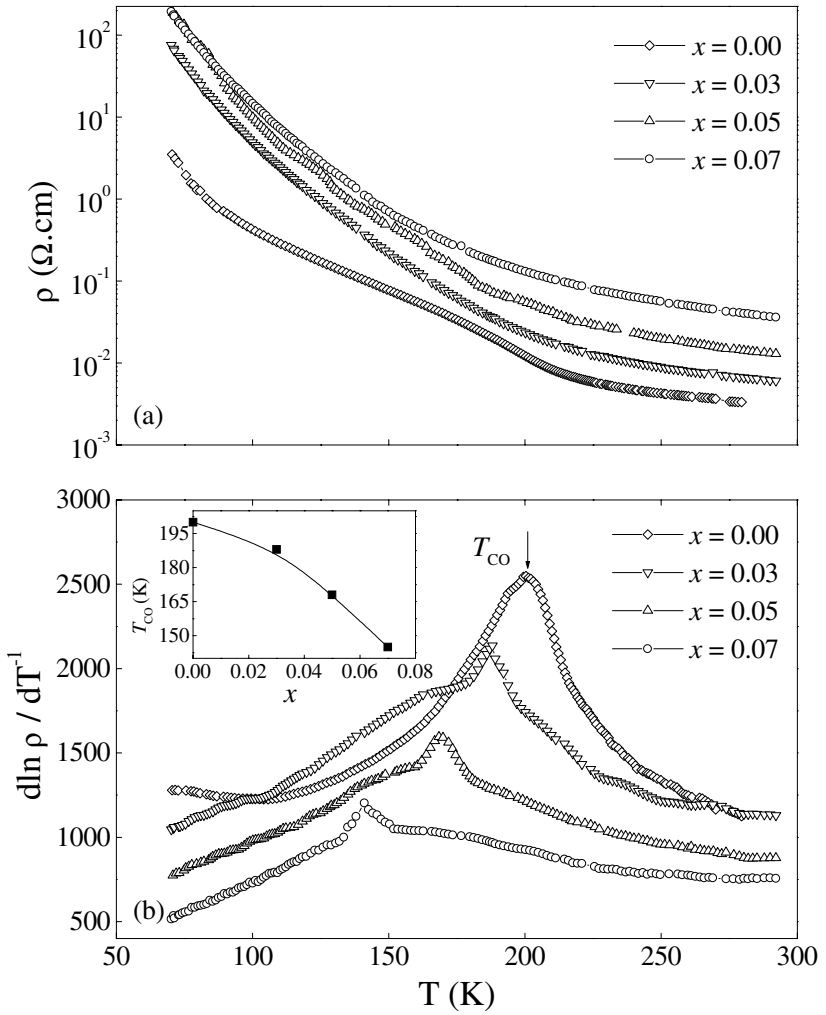

Figure 1. Variations of (a) the resistivity ρ and (b) the logarithmic derivative, $d(\ln \rho)/d(T^{-1})$, of the resistivity with temperature for $La_{0.25}Ca_{0.75}Mn_{1-x}Cr_xO_3$ ($x = 0$, 0.03, 0.05, and 0.07).

Mn^{3+}–O–Cr^{3+} interaction can result in an increase of the ferromagnetism of the system. In addition, the doped Cr acts as an impurity, hindering the establishing of antiferromagnetic charge ordering [13, 14]. All of these effects induced by substitution of Cr^{3+} for Mn^{3+} are strong enough to enhance the magnetization even at a low doping level of 7%.

Figure 4 shows the temperature dependencies of the longitudinal and transverse ultrasonic velocities (V_l and V_t). It can be seen that, for $T > T_{CO}$, both the longitudinal and transverse ultrasonic velocities are obviously softened as temperature decreases, and there is a minimum for V_l and V_t near T_{CO}. Below T_{CO}, both V_l and V_t show anomalous hardening and the relative changes of velocities $\Delta V/V_{min}$ become small with the increase of the Cr doping. It should be noted that $\Delta V/V_{min}$ is larger than 25% for all samples. This implies that there is a strong coupling via the J–T effect [15] in the system. The electron–phonon coupling below T_{CO} originates from the interaction between the carriers and the soft mode associated with the structural phase transition from a cubic to a tetragonal phase [6] with, locally, the character

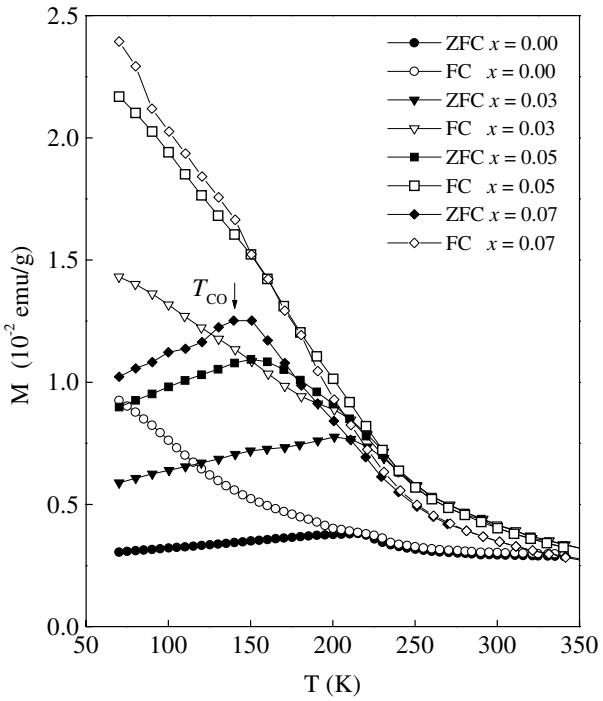

Figure 2. Variations of the zero-field-cooled (ZFC) and field-cooled (FC) magnetizations as functions of temperature for $La_{0.25}Ca_{0.75}Mn_{1-x}Cr_xO_3$ ($x = 0$, 0.03, 0.05, and 0.07).

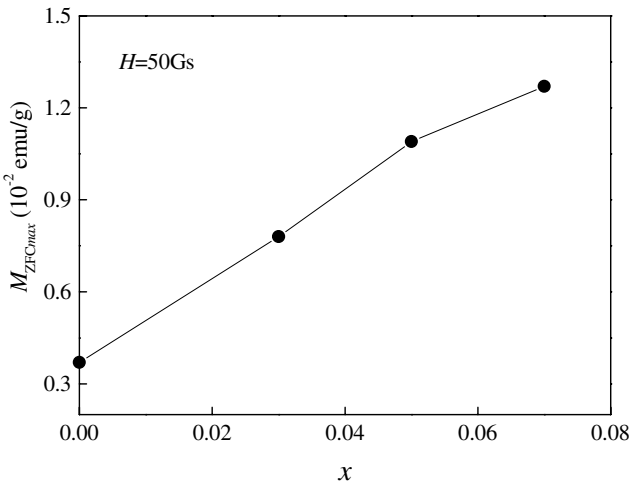

Figure 3. Maximum values of ZFC magnetizations as functions of Cr content. The line is a guide to the eyes.

of the octahedral tiltings or vibrations of the J–T type [16, 17]. From the measurements of ultrasonic velocities, one can obtain the shear modulus $G(T)$ as follows:

$$G(T) = DV_t^2 \tag{1}$$

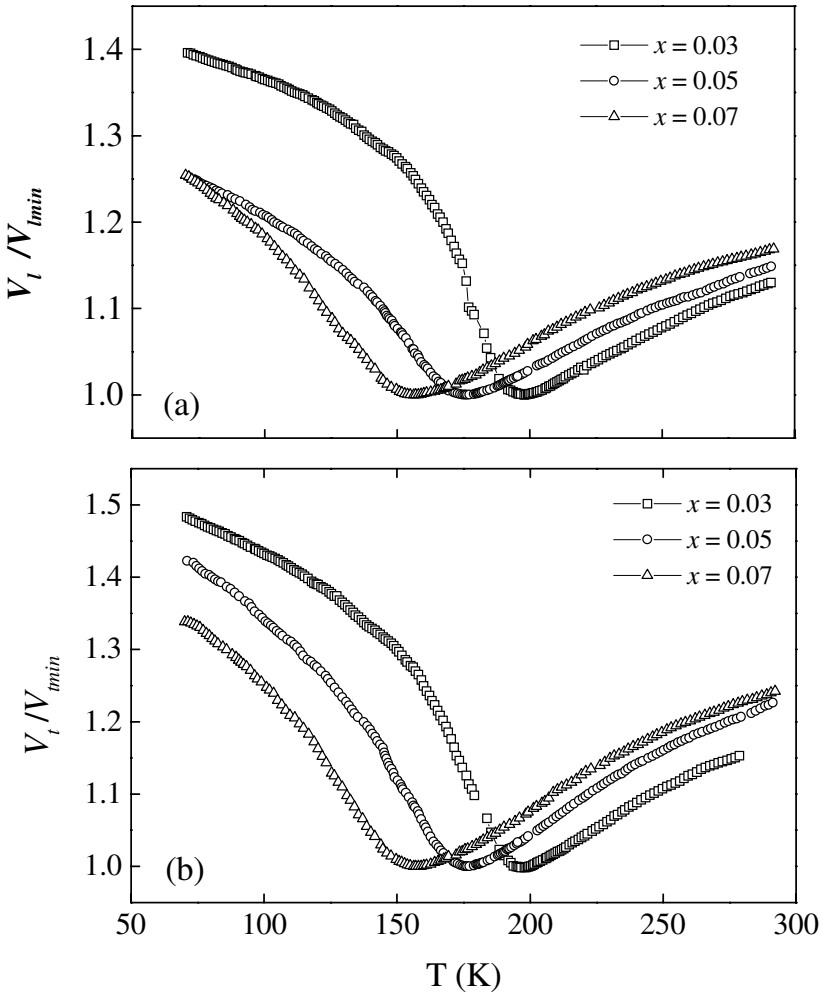

Figure 4. Ultrasonic velocities of $La_{0.25}Ca_{0.75}Mn_{1-x}Cr_xO_3$ ($x = 0.03, 0.05$, and 0.07) as functions of temperature. (a) The longitudinal velocity (V_l) and (b) the transverse velocity (V_t).

where D is the density of the system. Since there is a structural transition in the system around T_{CO}, the J–T effect is a cooperative one associated with the coupling of the J–T ions to distortions of the lattice. According to the cooperative J–T theory, one can give the relationship between $G(T)$ and temperature T [18] as follows:

$$\frac{G(T)}{G_0} = \left[1 - \frac{\lambda+\mu}{k_BT} + \frac{\lambda+\mu}{k_BT}\tanh^2\left(\frac{\Delta}{k_BT}\right)\right] \Big/ \left[1 - \frac{\lambda}{k_BT} + \frac{\lambda}{k_BT}\tanh^2\left(\frac{\Delta}{k_BT}\right)\right] \tag{2}$$

where G_0 is the shear modulus at absolute zero temperature, λ is the phonon exchange constant which is a composite measure of the effective coupling of all phonons of the appropriate symmetry to the Jahn–Teller ions, μ is a measure of the ion–strain coupling, and Δ is the J–T energy representing the effect of the ion–distortion coupling. For the charge-ordering transition, Δ can be written as [18]

$$\Delta = \Delta_0 \tanh\left(\frac{\Delta}{k_BT}\right)$$

where $\Delta_0 = k_B T_{CO}$ is the J–T energy at zero temperature (the values of Δ_0 are 16.21, 14.49, and 12.51 meV for $x = 0.03$, 0.05, and 0.07, respectively). When $T > T_{CO}$, corresponding to the undistorted, cubic, high-temperature phase, and $\Delta = 0$, one has the simple result

$$\frac{G(T)}{G_0} = \left(\frac{T - (\lambda + \mu)/k_B}{T - (\lambda/k_B)}\right) \qquad (T > T_{CO}). \tag{3}$$

Equation (2) and equation (3) can be used to fit the experimental data in the temperature ranges below and above T_{CO}, respectively. In figure 5, the open symbols are the experimental data and the solid lines are the results calculated using the parameters listed in table 1 for different Cr-doped samples. The decreases of Δ_0 and λ with increasing Cr content, shown in table 1, indicate that the electron–phonon interaction is weakened due to Cr doping. It should be pointed out that the theoretical calculations of the shear modulus deviate from the experiments in the temperature range around T_{CO}. Furthermore, the transition temperatures

$$T_C = \frac{\lambda + \mu}{k_B}$$

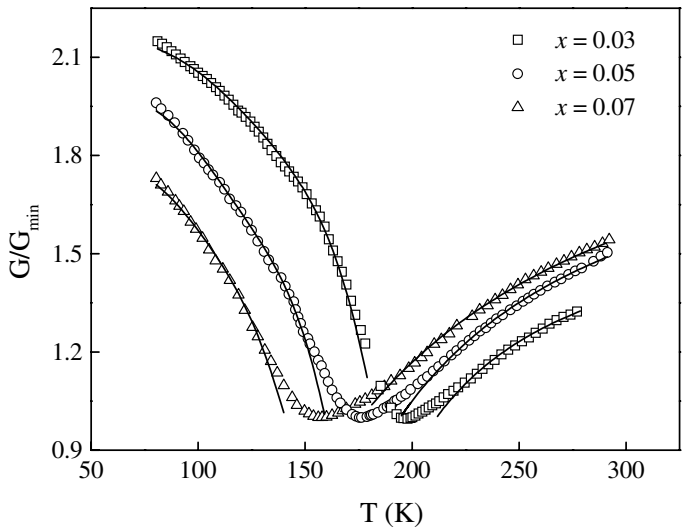

Figure 5. The temperature dependence of the shear modulus $G(T)$ of $La_{0.25}Ca_{0.75}Mn_{1-x}Cr_xO_3$ ($x = 0.03$, 0.05, and 0.07). Open symbols are experimental data; solid lines are results calculated using equation (2) at low temperature and equation (3) at high temperature.

Table 1. Fitting parameters for the shear modulus, using equation (2) at low temperature and equation (3) at high temperature, for $La_{0.25}Ca_{0.75}Mn_{1-x}Cr_xO_3$ ($x = 0.03$, 0.05, and 0.07) samples.

x	Temperature range	G_0/G_{min}	λ (meV)	$\lambda + \mu$ (meV)	Δ_0 (meV)
0.03	$80 < T < 180$ K	2.18	9.82	14.23	16.21
	$210 < T < 280$ K	1.71	11.39	14.23	—
0.05	$80 < T < 160$ K	2.05	6.49	12.08	14.49
	$195 < T < 290$ K	2.05	7.12	12.08	—
0.07	$80 < T < 140$ K	1.85	5.77	9.49	12.51
	$180 < T < 290$ K	2.22	2.41	9.49	—

deduced from λ and μ are about 165 K, 140 K, and 115 K for samples with Cr content $x = 0.03$, 0.05, and 0.07, respectively, and are smaller than the actual charge-ordering transition temperatures T_{CO}: 188 K, 168 K, and 145 K. The deviations between the experimental data and the theoretical results is probably due to the following two features. On the one hand, the critical fluctuation of the ion–distortion coupling related to the structure transition process may broaden the width of the transition of the shear modulus. On the other hand, around T_{CO} the system also experiences a magnetic transition which affects the ultrasonic properties.

The shift of T_{CO} to low temperature, and the decreases of the J–T energy and phonon exchange constant, induced by Cr doping can be regarded as due to one or more of the following features:

(i) According to Millis's polarization theory, the J–T effect originates from the splitting of e_g orbitals of Mn^{3+} ions, so Mn^{3+} is directly related to the distortion of the J–T effect. The substitution of Cr^{3+} for Mn^{3+} decreases the ratio of Mn^{3+} to Mn^{4+}, and the ion–distortion coupling of the J–T effect is thus weakened.

(ii) The strengthened ferromagnetism of the system favours destruction of the charge-ordering state, which has been confirmed by the fact that the CO state can be suppressed or destroyed in an external magnetic field [19, 20]. This result is consistent with those from many other studies of Cr-doped $R_{0.5}A_{0.5}MnO_3$ compounds which show that the effect of Cr doping on CO is similar to that of a magnetic field [14, 21].

In summary, our experimental results indicate that with increasing Cr content, the charge-ordering temperature T_{CO}, hardening of ultrasonic velocities, J–T energy, and phonon exchange constant decrease for $La_{0.25}Ca_{0.75}Mn_{1-x}Cr_xO_3$. All of these behaviours result from the weakening of the J–T effect via the electron–phonon coupling and the strengthened ferromagnetism induced by the substitution of Cr^{3+} for Mn^{3+} in the system. Our experiments suggest that the J–T energy is about 16.21–12.51 meV in the charge-ordered system.

Acknowledgment

This work was supported by the National Natural Science Foundation of China.

References

[1] Zener C 1951 *Phys. Rev.* B **82** 403
[2] Millis A J, Littlewood P B and Shraiman B I 1995 *Phys. Rev. Lett.* **74** 5144
[3] Ramirez A P, Schiffer P, Cheong S W, Chen C H, Bao W, Palstra T T M, Gammel P L, Bishop D J and Zegarski B 1996 *Phys. Rev. Lett.* **76** 3188
[4] Fernández-Díaz M T, Martínez J L, Alonso J M and Herrero E 1999 *Phys. Rev.* B **59** 1277
[5] Hejtmanek J, Jirak Z, Arnold Z, Marysko M, Krupicka S, Martin C and Damay F 1998 *J. Appl. Phys.* **11** 7204
[6] Li X G, Chen H, Zhu C F, Zhou H D, Zhen R K, Zhang J H and Chen L 2000 *Appl. Phys. Lett.* **76** 1173
[7] Zhao G M, Ghosh K, Keller H and Greene R L 1999 *Phys. Rev.* B **59** 81
[8] Argyriou D N, Bordallo H N, Campbell B J, Cheetham A K, Cox D E, Gardner J S, Hanif K, Dos Santos A and Strouse G F 2000 *Phys. Rev.* B **61** 15 269
[9] Varelogiannis G 2000 *Phys. Rev. Lett.* **85** 4172
[10] Jung J H, Lee H J, Noh T W, Choi E J, Moritomo Y, Wang Y J and Wei X 2000 *Phys. Rev.* B **62** 481
[11] Barnabe A, Maignan A, Hervieu M, Damay F, Martin C and Raveau B 1997 *Appl. Phys. Lett.* **71** 3907
[12] Raveau B, Maignan A and Martin C 1997 *J. Solid State Chem.* **130** 162
[13] Damay F, Maignan A, Martin C and Raveau B 1997 *J. Appl. Phys.* **82** 1485
[14] Kimura T, Kumai R, Okimoyo Y, Tomioka Y and Tokura Y 2000 *Phys. Rev.* B **62** 15 021
[15] Min B I, Lee J D and Youn S J 1998 *J. Magn. Magn. Mater.* **177–181** 881
[16] Zhao G M, Smolyaninova V, Prellier W and Keller H 2000 *Phys. Rev. Lett.* **84** 6086
[17] Podobedov V B *et al* 1999 *Appl. Phys. Lett.* **73** 3217

[18] Melcher R L 1970 *Physical Acoustics* vol 12, ed W P Mason (New York: Academic) p 19
[19] Kuwahara H, Tomioka Y, Asamitsu A, Moritomo Y and Tokura Y 1995 *Science* **270** 961
[20] Tomioka Y, Asamitsu A, Kuwahara H, Moritomo Y and Tokura Y 1996 *Phys. Rev.* B **53** R1689
[21] Moritomo Y, Machida A, Mori S, Yamamoto and Nakamura A 1999 *Phys. Rev.* B **60** 9220